Fluorescence Spectroscopic Properties and Single Aggregate Structures of π-Conjugated Wire-Type Dendrimers

Sadahiro Masuo, Hiroyuki Yoshikawa, Tsuyoshi Asahi, and Hiroshi Masuhara*

Department of Applied Physics and Frontier Research Center, Osaka University, Suita, Osaka 565-0871, Japan

Takafumi Sato, Dong-Lin Jiang, and Takuzo Aida

Department of Chemistry and Biotechnology, The University of Tokyo, Hongo, Bunkyo-ku, Tokyo 113-8685, Japan

Received: July 18, 2002; In Final Form: January 7, 2003

The spectroscopic properties of seven varieties of wire-type dendrimers, which consist of different generation numbers of dendritic wedges and molecular weights, were examined in tetrahydrofuran solution, in the solid state, and in good/poor solvent mixture for the purpose of revealing the relation between molecular conformation and spectral behavior. The second and third generation wire-type dendrimers showed a sharp aggregate band, which is ascribed to the interchain π stacked aggregate, in the solid state and in the good/poor solvent mixture, while the fourth generation wire-type dendrimer did not show the aggregate band. The absence of the aggregate band indicates that the bulky fourth generation dendritic wedges prevent the conjugated backbone from forming the interchain π stacked aggregate even in the solid state and in the good/poor solvent mixture. In the experiment on poor solvent-induced aggregation, we observed the progressive spectral change in the process of forming the aggregate, and simultaneously the aggregate formation was confirmed by observation of the fluorescence microscope image. The progressive spectral change suggested the molecular conformational change during the aggregate formation. Furthermore, the difference of molecular conformation depending on each aggregate and on some positions of the single aggregate was revealed using fluorescence microspectroscopy with the spatial resolution of about 1 μm.

Introduction

The wire-type dendrimers,[1] L*n*PPE*m* (*n* and *m* show the generation number of dendritic wedges and the average degree of polymerization (DP) of the rodlike backbone, respectively, and L*n*PPE without *m* indicates all the *n* generation wire-type dendrimers independent of *m*), consist of a rigid and fully conjugated poly(phenyleneethynylene) (PPE) backbone wrapped with flexible poly(benzyl ether) dendritic wedges. The chemical structures, the weight-average molecular weight (M_w), and its ratio to the number-average molecular weight (M_n), M_w/M_n, are listed in Figure 1 and Table 1. We have already applied these wire-type dendrimers to microscopic studies and have reported two topics as follows. (1) Molecular assemblies with different shapes are formed depending on the generation number and on DP upon casting on a glass substrate.[2] (2) Repetitive contraction and swelling behavior of gel-like wire-type dendrimer assemblies is controlled by photon force of a focused near-infrared laser beam.[3] In these two studies, fluorescence microspectroscopy has been utilized for analyzing molecular conformation and arrangement in the assemblies. Therefore, it is essential to investigate exactly the intrinsic spectroscopic properties of the wire-type dendrimers depending on the molecular conformation and spatial arrangements.

Since the original demonstrations of conjugated polymer light-emitting diodes (LEDs) by Partridge[4] and Burroughes et al.,[5] there continues to be great interest in achieving polymer device performance that rivals at inorganic or small molecule organic devices. In addition to LEDs, polymers have been demonstrated as the active material in a variety of electrooptic devices such as light-emitting electrochemical cells,[6] photodiodes,[7] lasers,[8] integrated circuits,[9] and polarizers for liquid-crystal displays.[10] PPE which is the backbone of the wire-type dendrimer and its derivatives are also the class of such polymers; therefore, spectroscopic properties of various PPEs have been investigated extensively in solutions and solid states, for example, molecular weight dependence and side chain effect for spectroscopic properties, intra- and interpolymer energy migration, and so on.[11−17] The spectroscopic properties of PPEs in dilute solution are relatively understood because only photophysical processes in a single polymer chain should be considered. Absorption spectra of PPEs show a typical broad band in the region of 350∼450 nm depending on DP and on the substituted position of side chains. About the relationship between absorption spectra and DP, Wautelet et al. studied ether-substituted PPE oligomers and polymers in tetrahydrofuran (THF) and reported that although the absorption peak wavelength was redshifted with increasing DP, its shift was saturated around 27 DP (27 phenylene rings).[12] In dilute solution, PPEs show a strong emission band and a second weaker shoulder with high quantum yield (Φ_{FL}). However, the Φ_{FL} value for PPEs of same constitution varies depending on their history, that is, synthesis route and so on, because it is influenced by small amount of impurities which are defect structures in the polymer chain.[13]

On the other hand, spectroscopic properties in solid state are more complicated because in addition to characteristics as a

* To whom all correspondences should be addressed. E-mail: masuhara@ap.eng.osaka-u.ac.jp.

10.1021/jp021643z CCC: $25.00
Published on Web 02/25/2003

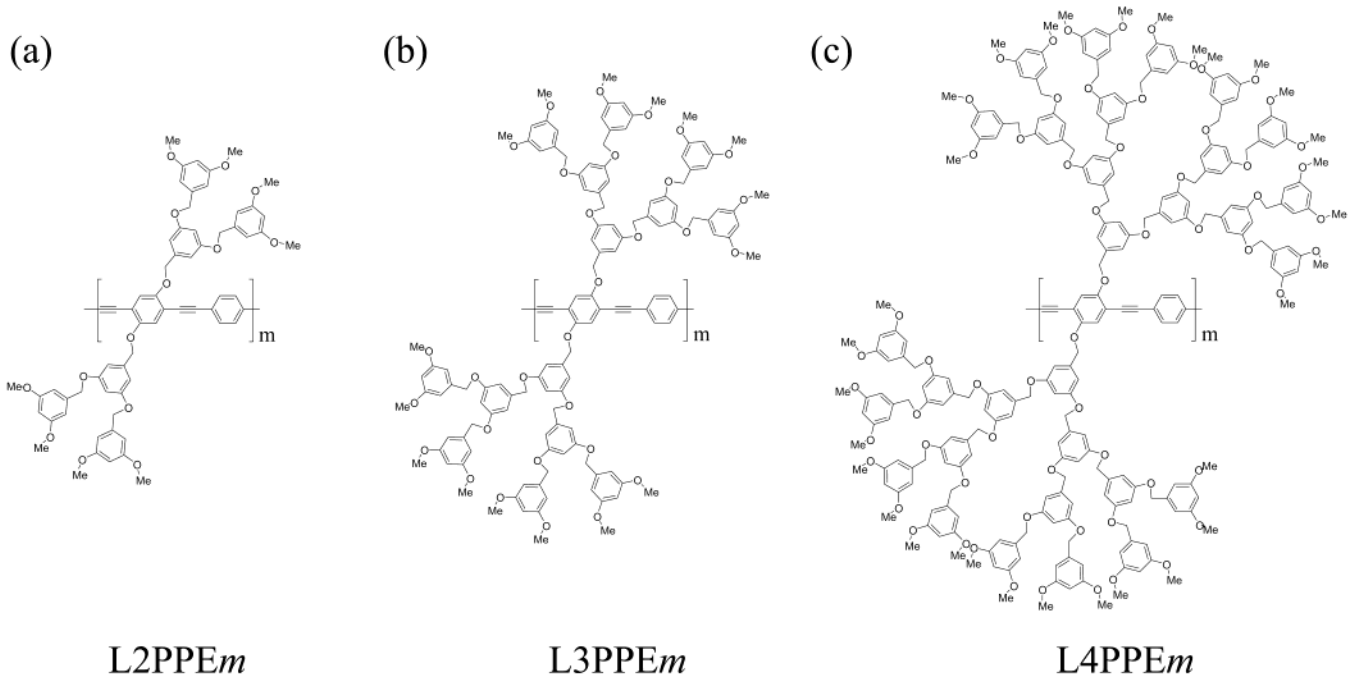

Figure 1. Chemical structures of the wire-type dendrimers, L*n*PPE*m*. *n* and *m* show the generation number of the dendritic wedges (the number of aromatic layers) and the degree of polymerization (DP) of PPE backbone, respectively. (a) L2PPE: second generation, (b) L3PPE: third generation, and (c) L4PPE: fourth generation.

TABLE 1: Weight-Average Molecular Weight (M_w) and Its Ratio to Number-Average Molecular Weight (M_n), M_w/M_n of Wire-Type Dendrimers

	M_w	M_w/M_n
L2PPE3	3400	1.1
L2PPE19	21500	3.4
L2PPE25	278000	2.5
L3PPE19	41700	1.6
L3PPE56	121800	2.5
L3PPE130	280000	6.5
L4PPE8	34000	1.5

single polymer chain in the solution, intermolecular interaction and molecular conformation and spatial arrangement realized in solid state have an immediate effect on the spectroscopic properties. Generally, a broad absorption band is redshifted compared to that in the solution, and a new sharp band appears at the long wavelength side of the broad band accompanying the formation of aggregates.[14−17] Therefore, the aggregate-induced new sharp band is observed also in good/poor solvent mixture, and the sharp band is called the "aggregate band". Two different explanations could be responsible for the observation of the aggregate band in PPEs. (a) The planarization of the conjugated backbone induced by forming aggregate leads to the increase of the conjugation length and thus to a lower band gap. (b) Interpolymer electronic interaction occurs by forming a tight-packing geometry of interchain π stacked aggregate. The fluorescence spectra in the solid state are redshifted and are broadened with lower Φ_{FL} as a result of fluorescence quenching[16−18] compared to those in the solution, and these fluorescence spectra are shown by superposition of plural different excited states which are attributed to aggregate state, excimer state, or long conjugated chain depending on the molecular conformation and spatial arrangement in the solid state. In addition, the reported data depend on the sample history, preparation of solid state samples, and research groups. Therefore, the intrinsic spectroscopic properties of the conjugated polymers have remained elusive, and the difficulties in obtaining such information are considered to be endemic to polymers. However, it is necessary and essential to investigate the intrinsic spectroscopic properties to analyze such molecular information in the microscopic level. Recently, Swager et al. have shown that the conformation of individual polymers and interpolymer interactions in conjugated polymers can be controlled through the use of Langmuir films of designed four surfactant building block PPEs. They showed that, by mechanically inducing reversible conformational changes of the Langmuir monolayers, the precious relationship between the intrinsic optical properties of the conjugated polymer and its single-chain conformation or interpolymer interactions could be obtained.[16]

We can also obtain the information of such a relationship, especially about the intermolecular interactions, by using seven varieties of wire-type dendrimers which consist of different generation numbers of the dendritic wedges and molecular weights, because intermolecular distance can be controlled by changing the generation number of dendritic wedges. Although PPEs possess high fluorescence quantum yields in dilute solution, their tendency to aggregate with increase of concentration leads to blue-green emission and to low fluorescence quantum yield as a result of fluorescence quenching.[16−18] One concept applied to avoid this detrimental π-aggregate behavior is concerned with incorporation of bulky side chains, namely, dendritic wedges. On the basis of this concept, some of the present authors synthesized wire-type dendrimers and reported that the large dendrimer framework in L4PPE encapsulated the conjugated backbone as an "envelope" and protected its photoexcited state from quenching. This was confirmed previously by measuring the concentration dependence of Φ_{FL} in THF solution.[1] We expect that the relationship between spectroscopic properties, molecular conformation, and spatial arrangement is revealed by comparison of each wire-type dendrimer in the solid state and in poor solvent-induced aggregate experiment. Except for these wire-type dendrimers, dendritic side-chain functionalization of several conjugated polymer systems has been synthesized in the use of poly(*p*-phenylenevinylene),[19] poly(fluorene),[20] poly(thiophene),[21] poly(triacetylene),[22] and poly(*p*-phenylene),[23] and in some dendritic

wedges−conjugated polymer systems, "enveloping effect" was investigated toward nonaggregate light-emitting polymer.[20]

Herein, we report spectroscopic properties of seven varieties of the wire-type dendrimers which consist of different generation numbers of dendritic wedges and molecular weights, mainly, aggregate/nonaggregate studies depending on the generation numbers in solid state and in good/poor solvent (THF/water) mixture for the purpose of efficient assignment of molecular conformation and space arrangement in the microscopic studies.

Experimental Section

π-Conjugated wire-type dendrimers, which the chemical structures and the associated data are listed in Figure 1 and Table 1, are used in the present work. THF (Nacalai Tesque, Spectro-Grade) was used without further purification as a good solvent. For measurements of absorption and fluorescence spectra in THF solution, a quartz cell, which optical pass length is 1 cm, was used. Solid-state samples of wire-type dendrimers were prepared on quartz substrates (22 mm × 30 mm) by casting and drying their THF solution in air at 21∼22 °C. The concentration of their THF solutions was adjusted by setting the absorbance at absorption maximum wavelength of the conjugated backbone (abs_{max}) to 0.30. In poor solvent-induced aggregation experiment, the wire-type dendrimers were dissolved in THF, which concentration was adjusted by setting abs_{max} to 0.10, and then absorption and fluorescence spectra were taken as water or methanol, a poor solvent, was gradually added to 3.0 mL of the THF solution.

Absorption and fluorescence spectra were measured by using UV−vis spectrometer (Shimadzu, UV-3100PC) and fluorescence spectrometer (Hitachi, F4500), respectively. In the fluorescence lifetime measurement, the second harmonic (λ = 390 nm, 150 fs, 76 MHz) of a mode-locked Ti:sapphire laser (Coherent, Mira 900 Basic) was used as an excitation light source, and fluorescence was detected by a ps streak camera (Hamamatsu Photonics). The concentration of the THF solutions was adjusted by setting abs_{max} to 0.10, then the solutions were bubbled with nitrogen gas. Fluorescence microscope images were acquired by using a conventional instrument (Olympus, universal fluorescence equipment) with a 40 x, 0.85 numerical aperture (N.A.) or a 100 x, 1.35 N.A. objective lens. Fluorescence spectra of a single aggregate were measured by using a ps fluorescence microspectroscopy system described elsewhere.[2]

Results and Discussion

I. In Solution. The absorption and fluorescence spectra of the wire-type dendrimers in THF solution are shown in Figure 2. The concentration of all THF solutions was adjusted by setting abs_{max} to 0.10, and fluorescence spectra were measured by the excitation at abs_{max}. All wire-type dendrimers showed an absorption band at 278 nm and a broad one at 300∼470 nm. The peak wavelengths of the absorption and fluorescence spectra are listed in Table 2. The absorption band at 278 nm is assigned to the dendritic wedges, so its contribution became relatively large with increasing the generation number of the dendritic wedges. Interestingly, upon excitation of these dendritic wedges at 278 nm in THF solution, only a blue fluorescence from the conjugated backbone was observed without any luminescence from the dendritic wedges, meaning that intramolecular singlet energy transfers from the dendrimer framework to the backbone chromophore units. The quantum efficiency of the intramolecular singlet energy transfer was estimated 100% independent of dendritic generation.[1] This energy transfer is one of the characteristic properties of wire-type dendrimers including other poly(benzyl ether) dendrimers.[24] The broad absorption bands are attributed to the conjugated backbone, and except for L2PPE3, the wavelengths of abs_{max} were invariant without depending on DP of the wire-type dendrimers. This means that the L2PPE3 whose DP is smaller than those of others has insufficient conjugation length in solution.

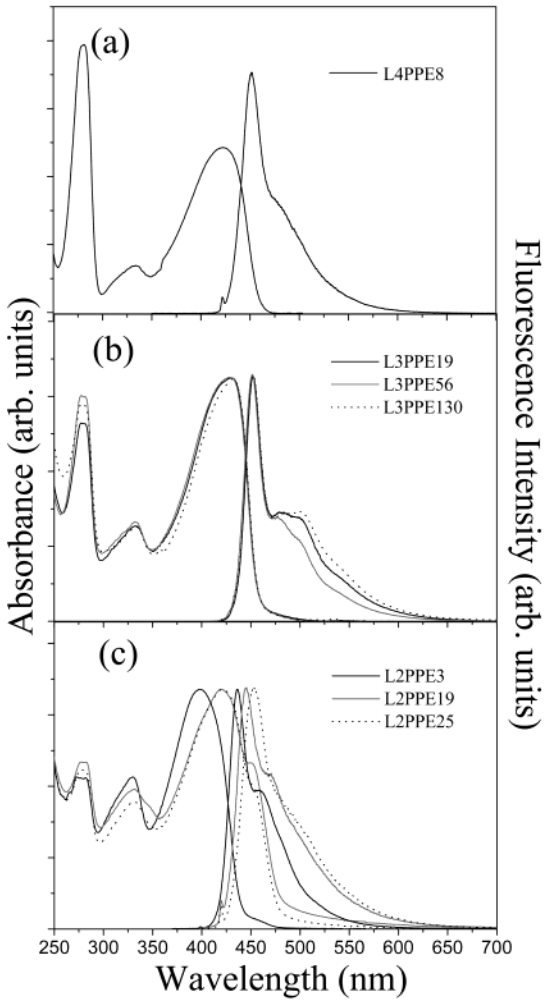

Figure 2. Absorption and fluorescence spectra of the wire-type dendrimers in THF solution. All fluorescence spectra were measured by excitation at abs_{max}. (a) L4PPE, (b) L3PPE, and (c) L2PPE.

TABLE 2: Peak Wavelengths at Absorption and Fluorescence Spectra of Wire-Type Dendrimers in THF Solution and Solid State[a]

	absorption		fluorescence	
	THF solution	solid state	THF solution	solid state
L2PPE3	278, 330, 400	278, 338, 440	436	470, 482, 502
L2PPE19	278, 330, 420	278, 338, 430, 457	445	475, 515
L2PPE25	278, 330, 420	278, 338, 436, 457	453	475, 515
L3PPE19	278, 332, 428	278, 338, 442, 470	453	478, 515
L3PPE56	278, 332, 428	278, 338, 442, 470	453	478, 515
L3PPE130	278, 332, 432	278, 340, 442, 470	453	478, 515
L4PPE8	278, 332, 423	278, 332, 435	451	468

[a] All wavelengths are given in nm.

On the other hand, fluorescence spectra of L2PPE were gradually redshifted with increasing DP. This redshift is the result of the increase in the π-conjugation length, and L4PPE, L3PPE, and L2PPE25 showed the fluorescence spectra around 453 nm. In the fluorescence spectra of L3PPE, a shoulder was observed around 500 nm, and this shoulder did not disappear even in more dilute solution (abs_{max}: below 0.01). The fact that

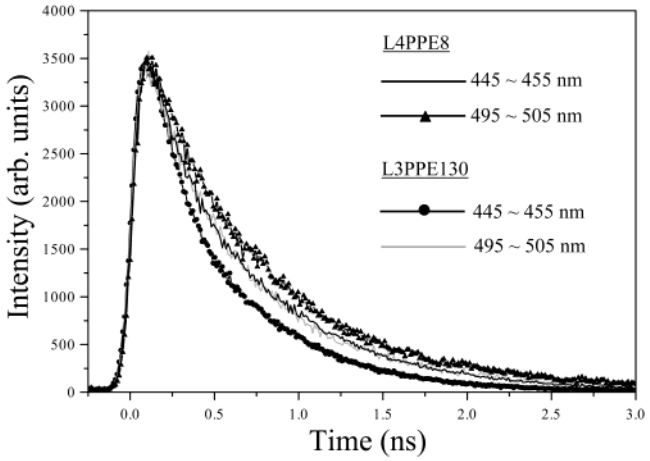

Figure 3. Fluorescence decay curves of L4PPE8 and L3PPE130 in THF solution. The concentration of the THF solution was prepared to give 0.10 at absorption maximum wavelength of conjugated backbone. Excitation wavelength was 390 nm. No excitation intensity dependence was observed.

the shoulder appeared in such a dilute solution indicates that plural different excited states exist in a single polymer chain; some of the present authors reported about Φ_{FL} as follows. Upon excitation of the conjugated backbone in dilute THF solution ($abs_{max} = 0.01$), L4PPE showed a strong blue fluorescence at 451 nm, where Φ_{FL} was evaluated to be virtually 100%. Of much interest is the fact that the Φ_{FL} value of L4PPE stayed at nearly 100% even when the solution was concentrated until the absorbance at abs_{max} was increased to 0.10. The fluorescence activity of the wire-type dendrimers is considerably dependent on the size of the dendritic wedges. Although the Φ_{FL} value of the one-generation smaller L3PPE was also very high under dilute condition (~100% at $abs_{max} = 0.01$), it showed a significant drop to 67% when the abs_{max} of the solution was increased to 0.10. Such a trend was more explicit in the lowest-generation L2PPE, where the Φ_{FL} value was only 56% even under dilute conditions ($abs_{max} = 0.01$) and further dropped upon increasing concentration of the solution.

From these observations, it was concluded that the large dendrimer framework in L4PPE encapsulated the conjugated backbone as an envelope and prevented its photoexcited state from quenching.[1] That is to say, it is considered that intermolecular interaction of L3PPE is absent in the concentration range where in the shoulder was observed; furthermore, no concentration dependence of fluorescence spectra was observed. Therefore, the shoulder observed in fluorescence spectra of L3PPE is attributed to another excited state in a single polymer chain. This assumption was clarified by the fluorescence lifetime measurement at different wavelengths. The fluorescence decay curves of L3PPE130 are shown in Figure 3. For comparison, those of L4PPE8 which showed a small contribution of the shoulder around 500 nm are also shown. These fluorescence decay curves were measured by the excitation at 390 nm. The concentration of the THF solutions was adjusted by setting abs_{max} to 0.10, then the solutions were bubbled with nitrogen gas. In L3PPE130, it can be seen that the fluorescence lifetime at 445~455 nm is shorter than that at 495~505 nm and relatively shorter than that of L4PPE8 in which such a monitor wavelength dependence of the fluorescence lifetime was also observed. This difference of the fluorescence lifetime suggests the existence of plural fluorescent species in a single polymer chain. The fluorescence decay curves of L4PPE8 and L3PPE130 could be fitted by a biexponential curve; therefore, it is considered that two fluorescence species which are probably

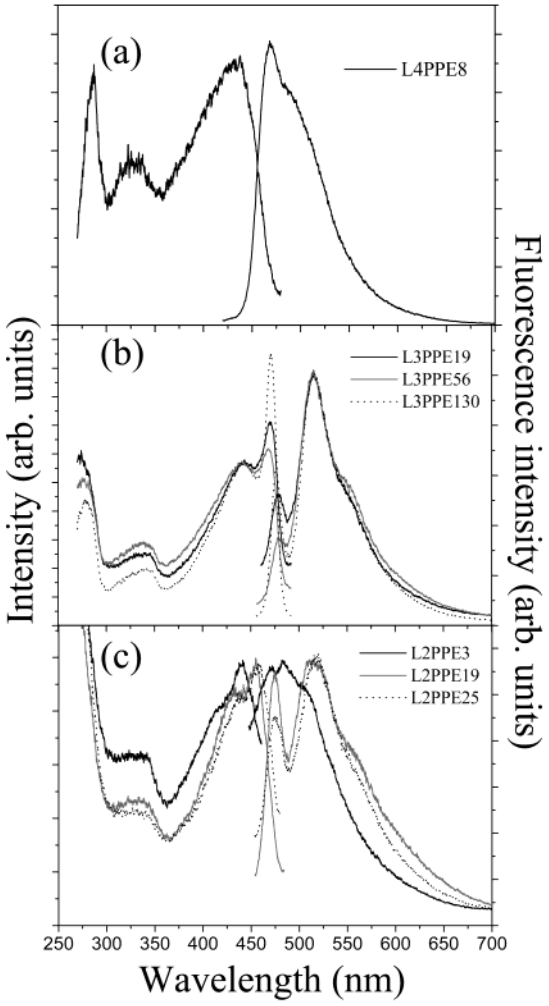

Figure 4. The fluorescence spectra and excitation spectra which were measured by monitoring around fluorescence maximum wavelengths of all wire-type dendrimers in solid state. (a) L4PPE, (b) L3PPE, and (c) L2PPE.

attributable to the different conjugation length exist in a single polymer chain of L4PPE8 and L3PPE130, and of course, intrachain energy migration[25] from the short chain to the long conjugation probably occur in a single polymer chain of these wire-type dendrimers, though no rise component could be observed with the time resolution of our apparatus.

II. Solid State. The fluorescence spectra and excitation ones which were measured by monitoring around fluorescence maximum wavelengths of all wire-type dendrimers in solid state are shown in Figure 4, and fluorescence microscope images of the solid-state samples are also shown in Figure 5. Interestingly, different shapes of the molecular assemblies depending on the generation numbers and DP were observed in the fluorescence microscope images. Its detailed investigation about the assembling structures has already been reported.[2] In Figure 4, excitation spectra are shown instead of their absorption spectra because the absorption spectra could not be measured clearly for the solid state. However, the peak wavelengths and the shapes of the excitation spectra almost coincided with those of the absorption spectra; furthermore, no monitor wavelength dependence of the excitation spectra was observed in all solid-state samples. L4PPE8 showed only a broad absorption spectrum (excitation spectra) and slightly broad fluorescence spectrum, which were redshifted by 12 and 17 nm relative to those in solution, respectively. On the other hand, in the excitation spectra, redshifted new sharp bands at 470 nm in L3PPE and

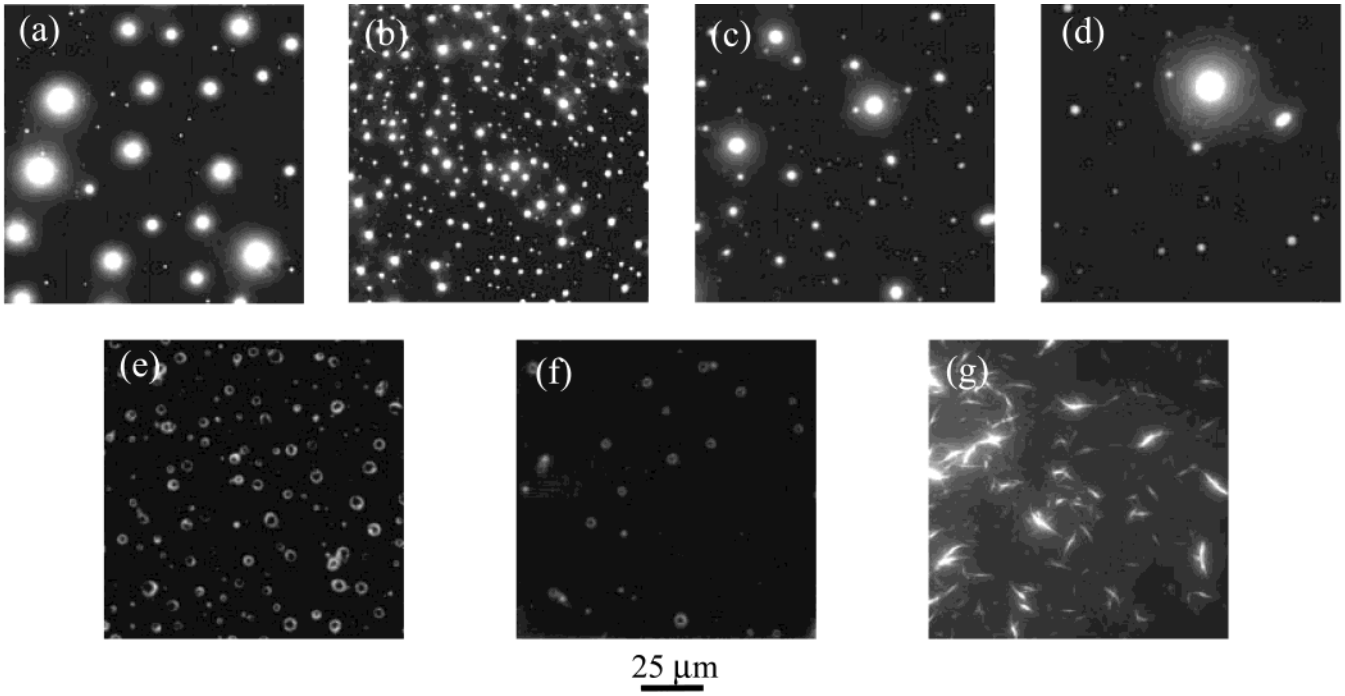

Figure 5. Fluorescence microscope images of solid-state samples on quartz substrate. (a) L4PPE8, (b) L3PPE130, (c) L3PPE56, (d) L3PPE19, (e) L2PPE25, (f) L2PPE19, and (g) L2PPE3. The scale bar below image f represents 25 μm.

at 457 nm in L2PPE19 and L2PPE25 appeared, and the broad bands were redshifted relative to those of the corresponding THF solutions. Accompanying the appearance of the redshifted new sharp band in the absorption spectra (excitation spectra), a new sharp band and a broad band at 478 and 517 nm, respectively, were observed in the fluorescence spectra of L3PPE. L2PPE19 and L2PPE25 also showed the same bands at 475 nm and 515 nm, respectively. It is considered that the redshifted new sharp absorption band corresponds to the new sharp fluorescence band, and the contributions of these bands in the spectra strongly depended on the preparation of the solid-state samples, although L3PPE, L2PPE19, and L2PPE25 showed such bands, invariably.

The redshifted new sharp absorption band is well known as an aggregate band of conjugated polymers.[14−17] As described above, two different explanations could be responsible for the observation of the aggregate band in PPEs. It is considered that no observation of the aggregate band in L4PPE8 is the result of preventing the conjugated backbone from interchain π stacking,[1] namely, the bulky fourth generation dendritic wedges encapsulate the conjugated backbone even in solid state. Thus, the observed spectral change from solution to solid state of L4PPE8 should be ascribed to intramolecular origin. We propose that these redshifts of the absorption and fluorescence spectra of L4PPE8 were attributed to the increase of the conjugation length by forming aggregate. However, in L3PPE and L2PPE which consist of smaller dendritic wedges than L4PPE, interchain π stacking could not be prevented; therefore, the aggregate band was observed in the solid state. We consider that the aggregate band is attributed not only to the planarization alone of a single molecule but also to interchain π stacking.[15−17] Of course, the planarization is also necessary for the interchain cofacial π stacking.

Detailed investigation about the relation between molecular conformation and spectral behavior is described below. It is considered that the sharp fluorescence spectra around 478 nm with small Stokes shift in L3PPE, L2PPE19, and L2PPE25 were emitted from the interchain π stacked aggregate state, and

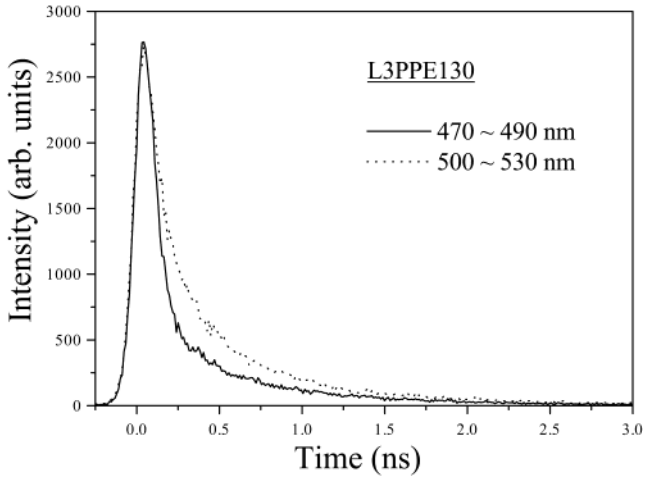

Figure 6. Fluorescence decay curves of L3PPE130 in solid state. Excitation wavelength was 390 nm.

broader bands at 515 nm are attributed to the longer conjugation part or other aggregate state. We can exclude the possibility of an excimer[26] because we clearly see a ground-state absorption that is responsible for the broad band, and the lifetime of the band is shorter than that of nonaggregated band of the THF solution. The fluorescence decay curves of L3PPE130 in solid state, which were measured at different wavelength, are shown in Figure 6. The fluorescence lifetime at 500∼530 nm which is attributed to the broad band is shorter than that in THF, and the lifetime of the aggregate band (470∼490 nm) is much shorter than that of the broad band.

III. Poor Solvent-Induced Aggregation Experiment. To investigate the relation between molecular conformation and spectral behavior in the process of forming π-stacked aggregate, we performed an experiment on poor solvent-induced aggregation which is similar to the literature.[14c,16] L4PPE8 and L3PPE130 were dissolved in THF, whose concentration was adjusted by setting abs_{max} to 0.10, and then absorption,

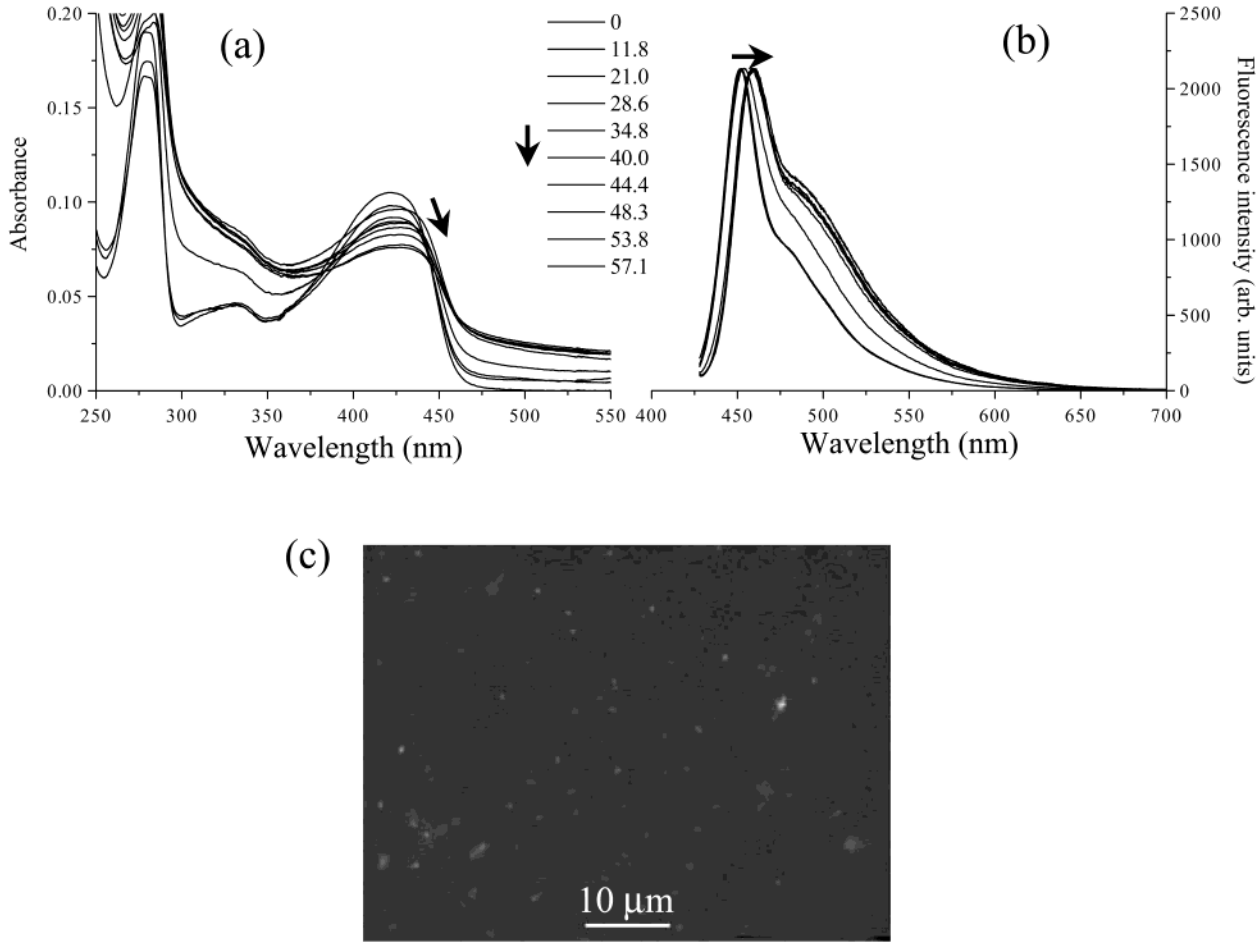

Figure 7. Absorption (a) and fluorescence spectra (b) of L4PPE8 in THF as function of added water. Inset values show content of water in %. The arrows indicate the decline or shift of bands with increasing water concentration. (c) Fluorescence microscope image of the induced aggregates of L4PPE8 in THF/water mixture. The scale bar in the image shows 10 μm.

fluorescence spectra, and fluorescence microscope images were taken by adding from time to time 0.2-mL portion of water, a poor solvent, to the 3-mL THF solutions. The spectra and fluorescence microscope images of L4PPE8 and L3PPE130 are shown in Figure 7 and Figure 8, respectively.

(a) L4PPE8. In the fluorescence image at 0% water content, only blue fluorescence from the solution was observed without aggregates. At 11.8% water content, blue aggregates started to form. As adding of water, the broad absorption band and the fluorescence spectra were gradually redshifted accompanying the aggregates formation (Figure 7c); simultaneously, the absorption spectrum was influenced by light scattering due to the aggregates. During the addition of water, only the small redshifts of the spectra were observed without appearance of a new band. At 57.1% water content, the peak wavelength of the broad absorption band and the fluorescence spectrum were redshifted by about 10 nm relative to its value at 0%. Further addition of water did not induce the spectral change anymore. This redshift is the result of the increase in π-conjugation length as a single polymer chain, which is induced by forming the aggregate. Although the wire-type dendrimers probably have nonplanar conformation in dilute THF solution, the formation of the aggregates leads to the planarization as a single polymer chain. Namely, the proximity of the wire-type dendrimer molecules induces the planarization, and the planar conformation can constitute a closed molecular packing. However, in L4PPE8, the close proximity of molecules is inhibited by the bulky dendritic wedges; therefore, aggregate band which is attributed to the interchain co-facial $\pi-\pi$ interaction was not observed. We could confirm the enveloping effect of bulky forth generation dendritic wedges again.

(b) L3PPE130. In the fluorescence image at 0% water content, only blue fluorescence from the solution was observed without aggregates, and then at 11.8%, small numbers of green fluorescent aggregates were observed; however, absorption and fluorescence spectra did not change because many molecules were dissolved in THF. A decrease in the absorbance is the result of concentration change of the solution. At 21.0% water content, a small redshift of the broad band was observed in the absorption spectra, and it can be seen that the absorption spectrum was influenced by light scattering due to the aggregates. In the fluorescence images, numerous green aggregates were observed (Figure 8c). At the same content, a broad band centered at 500 nm was prominent in the fluorescence spectrum. As increasing the water content, the redshift and the contribution of light scattering were observed remarkably in the absorption spectra, while more increase of 500 nm band was observed with declining the sharp band at 453 nm in the fluorescence spectra. At 40.0% water content, the broad band of the absorption spectra was redshifted by 10 nm relative to that at 0%, while the broad band at 500 nm became extremely large against the decrease of the sharp band at 453 nm in the fluorescence spectra. We consider that these spectral behaviors are attributed to the increase of the π-conjugation length accompanying the increased aggregation. However, the interchain π stacking is not formed at this stage because closer interchain distance is required for the formation of the π stacked aggregate. Therefore, further addition of water can induce the π stacked aggregate. Over

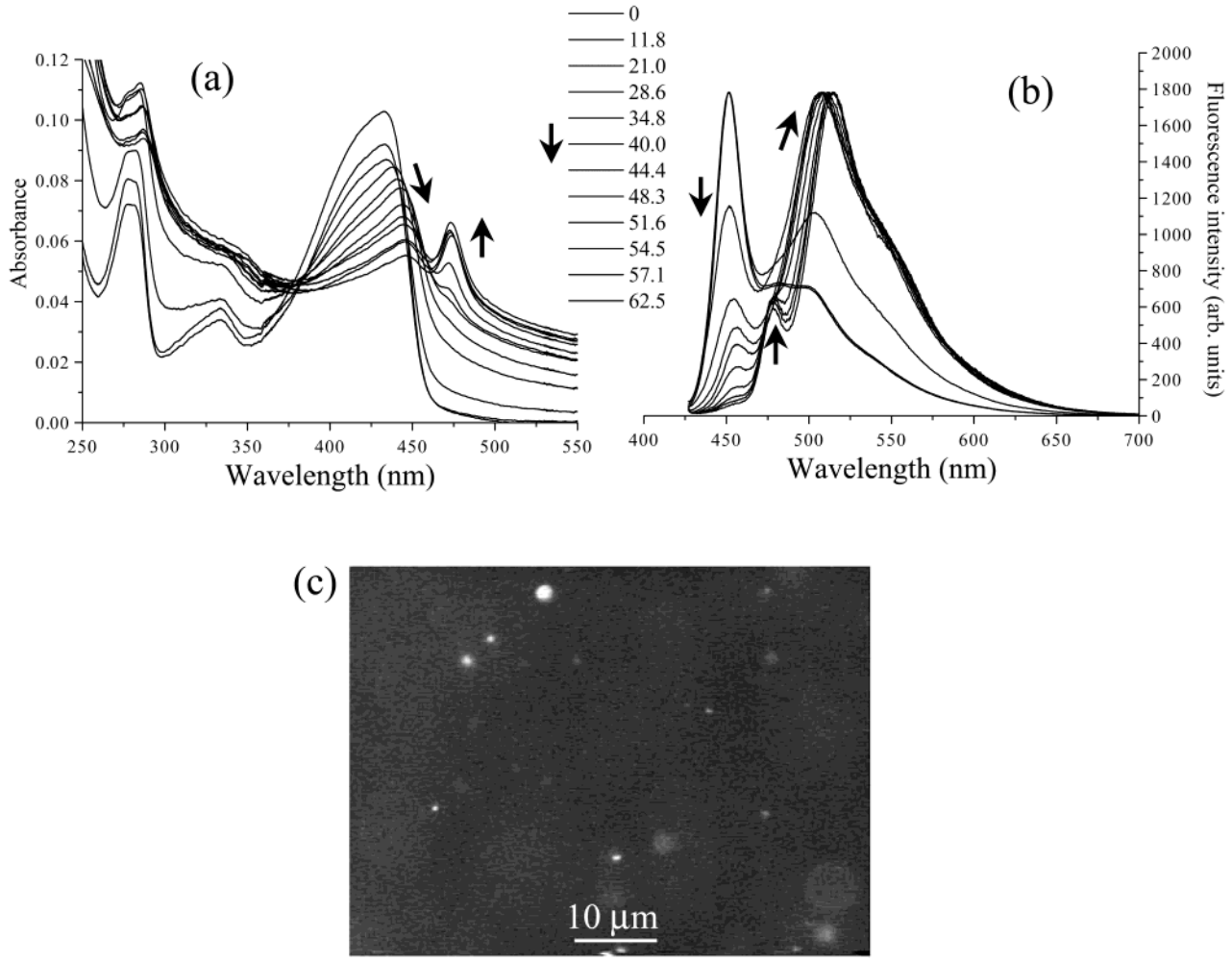

Figure 8. (a) Absorption and (b) fluorescence spectra of L3PPE130 in THF as function of added water. Inset values show content of water in %. The arrows indicate the growth, decline, or shift of bands with increasing water concentration. (c) Fluorescence microscope image of the induced aggregates of L3PPE130 in THF/water mixture. The scale bar in the image shows 10 μm.

44.4% water content, a new sharp band at 470 nm gradually appeared along with the redshift of the broad band in the absorption spectra, and simultaneously, a new sharp band at 478 nm also gradually appeared accompanying the redshift of the broad band in the fluorescence spectra. Around 57.1%, the contribution of the new sharp bands in the absorption and fluorescence spectra became maximum, and the broad absorption band was redshifted by 15 nm relative to that at 0%. Over 57.1%, further spectral change was not induced.

The peak wavelengths of these absorption and fluorescence spectra coincide with those of the spectra in the solid state. The sharp absorption band at 470 nm is the aggregate band, which is the result of interchain co-facial $\pi-\pi$ interaction as described at the fluorescence spectra in the solid state. Namely, closer proximity of planar wire-type dendrimer molecules induced the efficient formation of the interchain π staked aggregate. The spectral behavior during this poor solvent-induced aggregation experiment was also observed in the case of using methanol as poor solvent. During the poor solvent experiment, the change of the induced aggregate size could not be observed clearly. The sizes of aggregates were about 2 μm at maximum, and most aggregates were below 1 μm. It is difficult to estimate precise sizes from fluorescence microscope images; however, aggregate sizes of L3PPE130 were larger than that of L4PPE8. The difference of the fluorescence spectrum among the aggregate is revealed clearly by fluorescence microspectroscopy as described below.

IV. Fluorescence Microspectroscopy for Single Aggregates. Although the above spectroscopic measurement gave an averaged result for an ensemble of many aggregates, we can reveal the difference of the molecular conformation in each aggregate, furthermore, at some positions of a single aggregate by using confocal fluorescence microspectroscopy system with about 1 μm spatial resolution. We performed fluorescence microspectroscopic experiment for the solid-state sample of L4PPE8 (Figure 5a) and L3PPE130 (Figure 5b). As an excitation light source, the third harmonic (λ = 300 nm, 2 ps, 82 MHz) of a mode-locked Ti:sapphire laser was used, and a focal point for the single aggregate was controlled by the 3D piezo stage. Position dependence of the fluorescence spectra detected at single aggregates of L4PPE8 and L3PPE130 solid-state sample is shown in Figure 9. In L4PPE8, the fluorescence spectra which were detected from some positions of a single aggregate coincided in the peak wavelength and shape with each other, and these spectra were in agreement with the ensemble one. Furthermore, no spectral change was observed between single aggregates. Such an agreement of the fluorescence spectra means that each conjugated backbone of L4PPE8 is common in the aggregates because the backbone is encapsulated by the bulky forth generation dendritic wedges.

On the other hand, in L3PPE130, which consists of smaller third generation dendritic wedges, position dependence of the fluorescence spectra was observed. Figure 9b and c shows the fluorescence spectra detected from different two single ag-

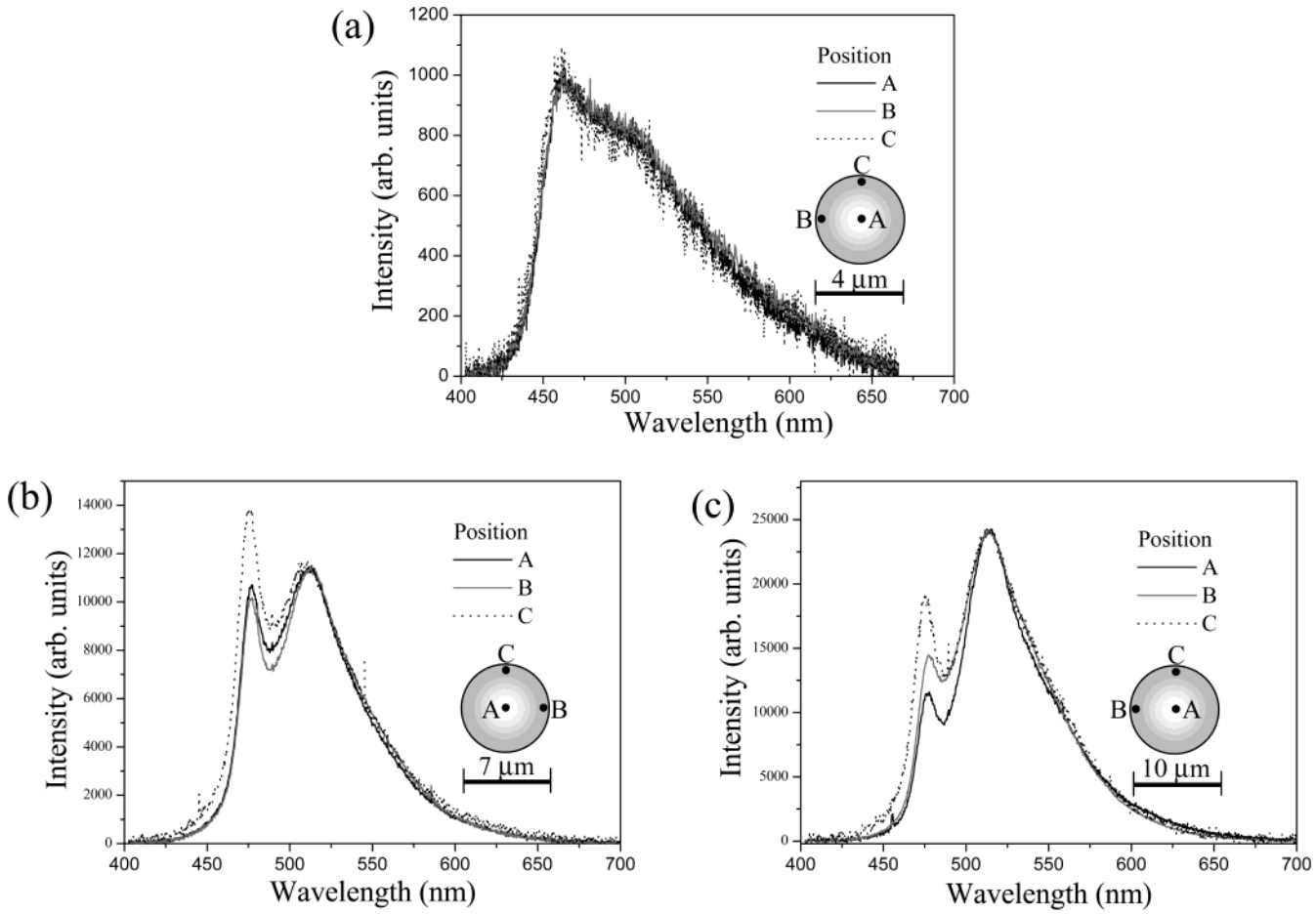

Figure 9. Position dependence of fluorescence spectra detected at single aggregates of L4PPE8 and L3PPE130 solid-state sample. (a) 4 μm sized aggregate of L4PPE8. (b) 7 μm sized aggregate of L3PPE130. (c) 10 μm sized aggregate of L3PPE130.

gregates, and it can be seen that the different contributions of the fluorescence sharp band at 478 nm were observed clearly, depending on the aggregates and on the positions of the aggregate. These fluorescence spectra were detected at the same distance from the aggregate surface; therefore, reabsorption effect is neglected. It is considered that the sharp band at 478 nm is attributed to the rigid π stacked aggregate; therefore, the observed different contributions of the fluorescence sharp band at 478 nm suggest that the conjugated backbone of L3PPE130 form different spatial arrangement in a single aggregate. This different molecular arrangement depending on the position in the single aggregate was also observed in the solid-state sample of L2PPE19 and L2PPE25. Interestingly, L4PPE8 and L3PPE130 formed the same-shaped (particle-like) aggregate in the solid state; nevertheless, molecular interaction in the aggregate of L4PPE8 was different from that in the aggregate of L3PPE130. Conjugated polymers such as alkyl-substituted PPE and alkyl-substituted polyfluorene form ordered (molecules are regularly oriented) ribbonlike aggregate in the solid state.[27,28] It is considered that in the wire-type dendrimer, bulky dendritic wedges and molecular length prevent fully co-facial stack structure, which is necessary for forming such an ordered ribbonlike structure. Therefore, L2PPE3, which consists of small dendritic wedges and short conjugated backbone, showed the tendency to form such a ribbonlike structure (Figure 5g).

Conclusions

Here, we have investigated spectroscopic properties of seven varieties of wire-type dendrimers, mainly, the relation between molecular conformation and spectral behavior depending on the generation number in solid state and in solvent/nonsolvent (THF/water) mixture for the purpose of efficient assignment of molecular conformation and space arrangement in the microscopic studies. In L2PPE and L3PPE, as the interchain distance decreased, namely, at the process of forming aggregates, progressive spectral changes were observed. This spectral behavior was attributed to nonplanarization, planarization, and interchain π stacked aggregate, progressively. Furthermore, in the solid-state sample, the difference of molecular conformation at each aggregate and at some positions of the aggregate was revealed using fluorescence microspectroscopy with about 1 μm spatial resolution. On the other hand, in the solid-state sample and nonsolvent-induced aggregation experiment of L4PPE8, the characteristic aggregate band was not observed in its absorption spectra. The absence of the aggregate band indicates that the bulky fourth generation dendritic wedges prevent the conjugated backbone from forming the interchain π stacked aggregate. This interpretation of the relation between spectral behavior and molecular conformation will be useful for determining the molecular conformation and association, for example, in the characteristic molecular assembly which is formed by photon force of a focused near-infrared laser beam.

Acknowledgment. The present work is partly supported by the Grant-in Aid for Scientific Research (KAKENHI)(s) (14103006) from Japan Society for the Promotion of Science.

References and Notes

(1) Sato, T.; Jiang, D.-L.; Aida, T. *J. Am. Chem. Soc.* **1999**, *121*, 10658.
(2) Masuo, S.; Yoshikawa, H.; Asahi, T.; Masuhara, H.; Sato, T.; Jiang, D.-L.; Aida, T. *J. Phys. Chem. B* **2001**, *105*, 2885.

(3) Masuo, S.; Yoshikawa, H.; Asahi, T.; Masuhara, H.; Sato, T.; Jiang, D.-L.; Aida, T. *J. Phys. Chem. B* **2002**, *106*, 905.
(4) Partridge, R. H. *Polymer* **1983**, *24*, 755.
(5) Burroughes, J. H.; Bradley, D. D. C.; Brown, A. R.; Marks, R. N.; Mackay, K.; Friend, R. H.; Burns, P. L.; Holmes, A. B. *Nature* **1990**, *347*, 539.
(6) Pei, Q. B.; Yu, G.; Zhang, C.; Yang, Y.; Heeger, A. J. *Science* **1995**, *269*, 1086.
(7) Yu, G.; Wang, J.; McElvain, J.; Heeger, A. J. *Adv. Mater*. **1998**, *10*, 1431.
(8) (a) Hide, F.; Diaz-Garcia, M. A.; Schwartz, B. J.; Heeger, A. J. *Acc. Chem. Res.* **1997**, *30*, 430. (b) Hide, F.; Schwartz, B. J.; Diaz-Garcia, M. A.; Heeger, A. J. *Chem. Phys. Lett*. **1996**, *256*, 424.
(9) Sirringhaus, H.; Tessler, N.; Friend, R. H. *Science* **1998**, *280*, 1741.
(10) (a) Palmans, A. R. A.; Smith, P.; Weder, C. *Macromolecules* **1999**, *32*, 4677. (b) Weder, C.; Sarwa, C.; Montali, A.; Bastiaansen, C.; Smith, P. *Science* **1998**, *279*, 835.
(11) (a) Walters, K. A.; Ley, K. D.; Schanze, K. S. *Langmuir* **1999**, *15*, 5676. (b) Yang, J. S.; Swager, T. M. *J. Am. Chem. Soc*. **1998**, *120*, 11864. (c) Yang, J. S.; Swager, T. M. *J. Am. Chem. Soc*. **1998**, *120*, 5321. (d) Kloppenburg, L.; Song, D.; Bunz, U. H. F. *J. Am. Chem. Soc*. **1998**, *120*, 7973. (e) Li, H.; Powell, D. R.; Hayashi, R. K.; West, R. *Macromolecules* **1998**, *31*, 52. (f) Giesa, R. *J. Macromol. Sci. Rev., Macromol. Chem. Phys*. **1996**, *C36*, 631. (g) Weder, C.; Wrighton, M. S. *Macromolecules* **1996**, *29*, 5157. (h) Moroni, M.; Le Moigne, J.; Luzzati, S. *Macromolecules* **1996**, *29*, 5157. (i) Mangel, T.; Eberhardt, A.; Scherf, U.; Bunz, U. H. F.; Müllen, K. *Macromol. Rapid. Commun.* **1995**, *16*, 571. (j) Moroni, M.; Le Moigne, J.; Luzzati, S. *Macromolecules* **1994**, *27*, 562.
(12) Wautelet, P.; Moroni, M.; Oswald, L.; Le Moigne, J.; Pham, A.; Bigot, J.-Y.; Luzzati, S. *Macromolecules* **1996**, *29*, 446.
(13) Bunz, U. H. F. *Chem. Rev.* **2000**, *100*, 1605.
(14) (a) Miteva, T.; Palmer, L.; Kloppenburg, L.; Neher, D.; Bunz, U. H. F. *Macromolecules* **2000**, *33*, 652. (b) Fiesel, R.; Halkyard, C. E.; Rampey, M. E.; Kloppenburg, L.; Studer-Martinez, S. L.; Scherf, U.; Bunz, U. H. F. *Macromol. Rapid Commun*. **1999**, *20*, 107. (c) Halkyard, C. E.; Rampey, M. E.; Kloppenburg, L.; Studer-Martinez, S. L.; Bunz, U. H. F. *Macromolecules* **1998**, *31*, 8655.
(15) (a) Kim, J.; McQuade, D. T, McHugh, S. K.; Swager, T. M. *Polym. Prepr*. **2000**, *41*, 32. (b) Levitsky, I. A.; Kim, J.; Swager, T. M. *J. Am. Chem. Soc*. **1999**, *121*, 1466.
(16) Kim, J.; Swager, T. M. *Nature* **2001**, *411*, 1030.
(17) (a) Kim, J.; McQuade, D. T.; McHugh, S. K.; Swager, T. M. *Angew. Chem., Int. Ed.* **2000**, *39*, 3868. (b) McQuade, D. T.; Kim, J.; Swager, T. M. *J. Am. Chem. Soc.* **2000**, *122*, 5885.
(18) (a) Samuel, I. D. W.; Rumbles, G.; Collison, C. J. *Phys. Rev. B* **1995**, *52*, R11573. (b) Jenekhe, S. A.; Osaheni, J. A. *Science* **1994**, *265*, 765.
(19) Bao, Z.; Amundson, K. R.; Lovinger, A. J. *Macromolecules* **1998**, *31*, 8647.
(20) (a) Setayesh, S.; Grimsdale, A. C.; Weil, T.; Enkelmann, V.; Müllen, K.; Meghdadi, F.; List, E. J. W.; Leising, G. *J. Am. Chem. Soc*. **2001**, *123*, 946. (b) Marsitzky, D.; Vestberg, R.; Blainey, P.; Tang, B. T.; Hawker, C. J.; Carter, K. R. *J. Am. Chem. Soc.* **2001**, *123*, 6965.
(21) Malenfant, P. R. L.; Fréchet, J. M. J. *Macromolecules* **2000**, *33*, 3634.
(22) Schenning, A. P. H. J.; Martin, R. E.; Ito, M.; Diederich, F.; Boudon, C.; Gisselbrecht, J.-P.; Gross, M. *Chem. Commun.* **1998**, 1013.
(23) (a) Schlüter, A. D.; Rabe, J. P. *Angew. Chem., Int. Ed.* **2000**, *39*, 864. (b) Bo, Z.; Zhang, C.; Severin, N.; Rabe, J. P.; Schlüter, A.-D. *Macromolecules* **2000**, *33*, 2688. (c) Karakaya, B.; Claussen, W.; Gessler, K.; Saenger, W.; Schlüter, A.-D. *J. Am. Chem. Soc*. **1997**, *119*, 3296.
(24) (a) Wakabayashi, Y.; Tokeshi, M.; Hibara, A.; Jiang, D.-L.; Aida, T.; Kitamori, T. *J. Phys. Chem. B* **2001**, *105*, 4441. (b) Jiang, D.-L.; Aida, T. *J. Am. Chem. Soc*. **1998**, *120*, 10895.
(25) (a) Schwartz, B. J.; Nguyen, T.-Q.; Wu, J.; Tolbert, S. H. *Synth. Met.* **2001**, *116*, 35. (b) Yu, J.; Hu, D.; Barbara, P. F. *Science* **2000**, *289*, 1327. (c) Chen, L. X.; Jäger, W. J. H.; Niemczyk, M. P.; Wasielewski, M. R. *J. Phys. Chem. A* **1999**, *103*, 4341. (c) Swager, T. M. *Acc. Chem. Res.* **1998**, *31*, 201. (d) Yip, W.-T.; Hu, D.; Yu, J.; Vanden Bout, D. A.; Barbara, P. F. *J. Phys. Chem. A* **1998**, *102*, 7564. (e) Vanden Bout, D. A.; Yip, W.-T.; Hu, D.; Fu, D.-K.; Swager, T. M.; Barbara, P. F. *Science* **1997**, *277*, 1074. (f) Zhou, Q.; Swager, T. M. *J. Am. Chem. Soc.* **1995**, *117*, 7017. (g) Swager, T. M.; Gil, C. J.; Wrighton, M. S. *J. Phys. Chem.* **1995**, *99*, 4886.
(26) Conwell, E. *Trends. Polym. Sci.* **1997**, *5*, 218.
(27) (a) Leclère, P.; Calderone, A.; Marsitzky, D.; Francke, V.; Geerts, Y.; Müllen, K.; Brédas, J. L.; Lazzaroni, R. *Adv. Mater.* **2000**, *12*, 1042. (b) Samori, P.; Francke, V.; Müllen, K.; Rabe, J. P. *Chem. Eur. J*. **1999**, *5*, 2312.
(28) Teetsov, J. A.; Vanden Bout, D. A. *J. Am. Chem. Soc*. **2001**, *123*, 3605.